

Proceedings of the Eurosensors XXIII conference

MEMS Stage Integrated with Microlens Arrays for High-Resolution Beam Steering

Sertan Kutal Gokce^{a*}, Sven Holmstrom^a, Cyrille Hibert^b, Caglar Ataman^c, Aslihan Arslan^a, Huseyin R. Seren^a, Hakan Urey^a

^aElectrical Engineering Department, KOC University, 34450 Istanbul, Turkey

^bCentre of Microfabrication, École Polytechnique Fédérale de Lausanne, 1015 Lausanne, Switzerland

^cSAMLAB, École Polytechnique Fédérale de Lausanne, Neuchâtel, Switzerland

Abstract

A novel micromechanical stage with a uniaxial set of combfingers capable of 2D actuation is designed and developed. Driven at resonance the stage deflects up to 108µm out-of-plane and 102µm in-plane, with 140V and 94V peak-to-peak actuation voltage, respectively.

Keywords: Hybrid integration; Comb drive; Beam steering

1. Introduction

In recent years there has been an increasing focus on laser scanning systems designed for restrictive form factors, such as endoscopic in situ imaging and compact projection display systems [1]. The bulk of these systems utilize mirrors to steer the beam and thus require beam folding. It has been demonstrated that an arrangements of two microlens arrays (MLA) separated by two focal lengths without any folding of the beam can be used to achieve large angle beam steering with only very small lateral displacements of one of the arrays [2,3]. This leads to the possibility of creating imaging systems with small cross sections. Microelectromechanical systems (MEMS) have earlier been utilized for beam steering with individual microlenses [4, 5]. The specific application motivating this work is high-resolution beam steering for an endoscopic laser imaging camera that can fit inside a 5 mm diameter

* Corresponding author. Tel.: +90 212 338 1772 ; fax: +90 212 338 1548.

E-mail address: sergokce@ku.edu.tr.

tube. To address this need a novel micromechanical stage with a uniaxial set of combfingers capable of 2D actuation is developed. The 2D stage is furthermore integrated with a vertically mounted microlens array to enable laser beam steering applications.

2. Device properties

The devices were fabricated on Silicon-On-Isolator (SOI) wafers with a device layer of $50\mu\text{m}$. The device consists of two cascaded frames, each suspended by four flexures (see Fig. 1.). The dimensions of the outer frame are $4.2\text{mm} \times 2.0\text{mm}$ and its four flexures are all parallel to its longer side, each $800\mu\text{m}$ long and $10\mu\text{m}$ wide. The inner frame is $300\mu\text{m} \times 1150\mu\text{m}$ and is suspended by two straight and two folded flexures. The straight flexures are each $850\mu\text{m}$ and are parallel to the outer flexures, while the folded flexures are $800\mu\text{m}$. The four inner flexures are $12\mu\text{m}$. The process flow of the three mask fabrication is given in Fig. 2. Mask 1 is used for patterning of gold pads for wire bonding and electrical connections; Mask 2 is used for front side device definition; Mask 3 is for back side opening and device release. As a starting point, a $50\mu\text{m}$ device layer SOI wafer is used. For electrical connections, an Au/Cr layer (130/15nm) is sputtered on the device side of the wafer (Fig. 2.2). The metal layers are patterned through wet etch (Fig. 2.3). Next step is to define front side device definition with deep reactive ion etch (DRIE) (Fig. 2.4). Backside photolithography is then done using Mask 3. Following this a second DRIE step is performed to create the device backside openings and dice trenches (Fig. 2.5). Finally, the devices are released with HF vapor phase etch (Fig. 2.6). The hybrid integration of MLAs on top of MEMS stages is performed manually after the fabrication of the stages with the help of a set of microstages (Fig. 2.7). The lens is attached to the inner frame of the device with UV-curable epoxy. The integration of the MLA array with the MEMS stage is illustrated in Fig. 1.

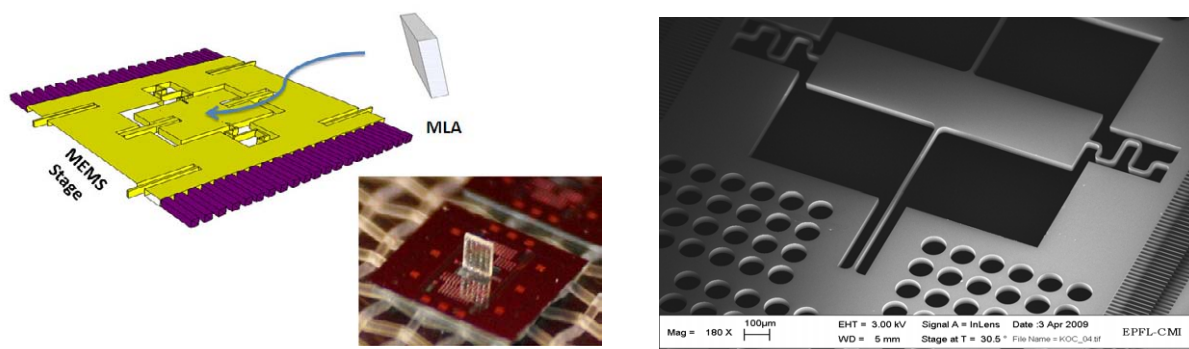


Fig. 1. To the left an illustration of hybrid MLA integration and a MLA integrated MEMS stage. To the right, a scanning electron microscopy image of the empty stage.

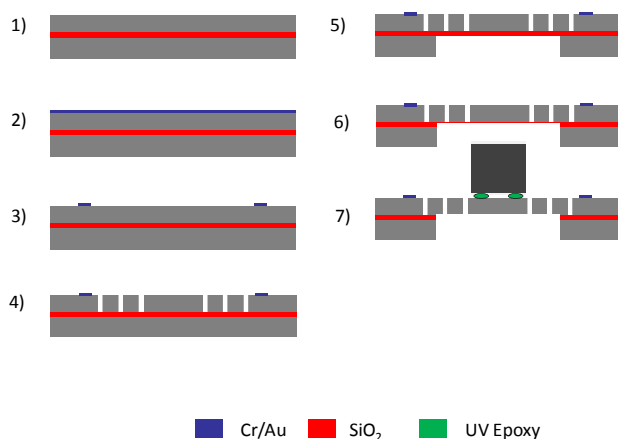


Fig. 2. Process flow for the 2D actuator stages.

Fig. 1. shows the fabricated MEMS stage. There are four springs connecting the inner stage to the outer moving frame, which is also suspended by 4 flexures. As seen in the SEM picture, there are holes on the front side designed to decrease the frame weight and increase the quality factor for the resonant out of plane motion. FEM modeling of the lone 2D actuated MEMS stage predict the in-plane and out-of-plane vibration frequencies at 1356Hz and 5800Hz. In-plane motion axis is designed to be linear and controlled at low-frequencies. The out-of-plane axis is resonant and actuated using mechanical coupling principle [6, 7].

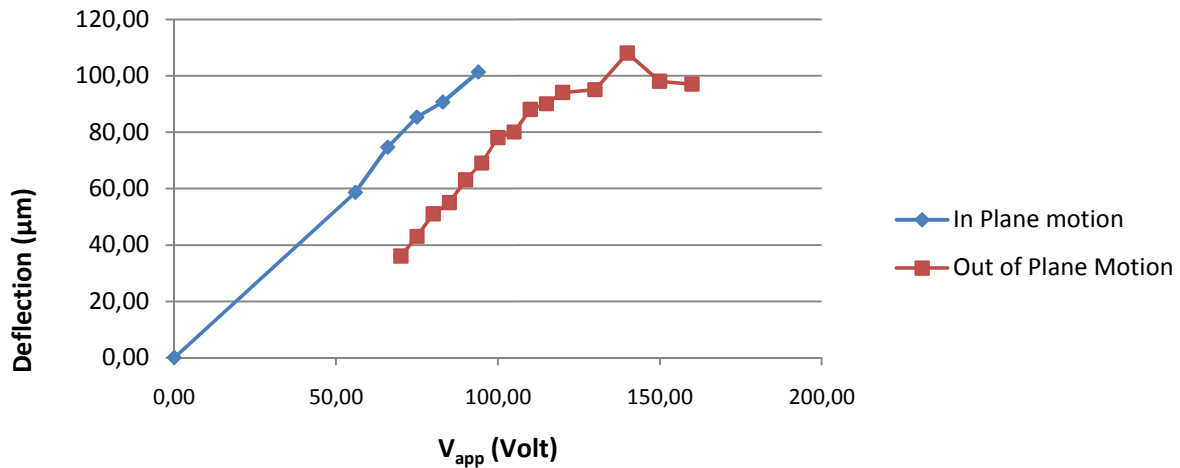


Fig. 3. Peak-to-peak displacement versus peak-to-peak voltage at resonance for in-plane and out-of-plane resonance modes. For this measurement the two modes are individually actuated. The data of the out-of-plane motion does not start from zero due to the parametric nature of this mode.

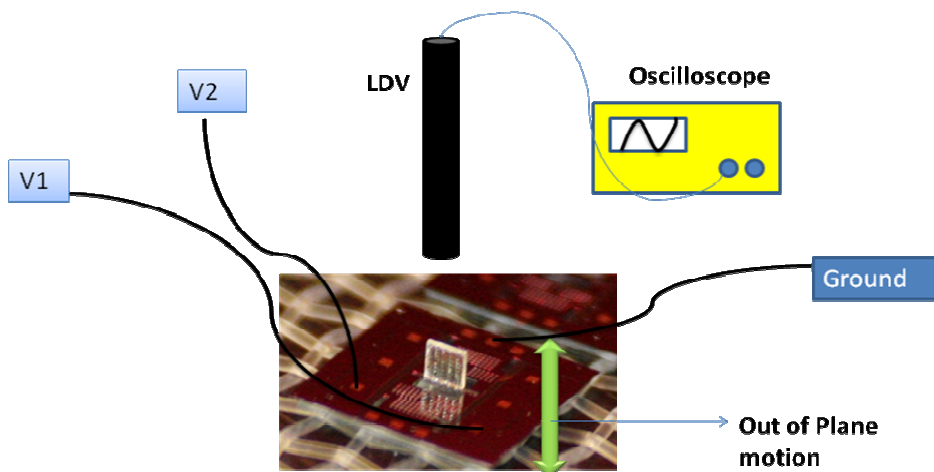


Fig. 4. The devices were actuated by connecting the moving parts to ground and applying voltages V_1 and V_2 , respectively to the two fixed comb sets. Measurements were done with LDV for the out-of-plane motion and from camera output for the in-plane motion.

3. Results

Experimental data of the MEMS stage without MLA are given in Fig. 3. The out-of-plane motion is measured with laser doppler vibrometry (LDV) and the in-plane motion from camera output. For the data presented here the two modes were actuated separately. Details of the measurement setup are described in Fig. 4. The respective signals used for out-of-plane and in-plane actuation are:

$$\text{Out-of-plane: } V_1 = V_2 = V_{app}(1 + \sin \omega t) \quad (1)$$

$$\text{In-plane: } V_1 = V_{app}(1 + \sin \omega t), V_2 = V_{app}(1 - \sin \omega t) \quad (2)$$

As can be seen in Fig. 3, the data for the out-of-plane mode does not reach zero. This is due to the parametric nature of this mode [8]. During experiments, approximately 102 μm peak-to-peak deflection of in-plane motion is obtained at resonance with 94V peak-to-peak. For the out-of-plane mode, 108 μm peak-to-peak deflection of inner frame is obtained at resonance with 140V peak-to-peak.

Acknowledgements

All the micro-fabrication in this work was performed at Center of Microtechnology (CMI) at EPFL, Lausanne, Switzerland with the support of the CMI-staff. Furthermore, the authors would also like to acknowledge Jean-Baptiste Bureau for contributions to the process development, Philippe Fluckiger and Yusuf Leblebici for support and help and Selim Olcer for help with measurements. This work was supported by TUBITAK under project 106E068.

References

1. Ra H, Piyawattanametha W, Taguchi Y, Lee D, Mandella MJ, Solgaard O. Two-dimensional MEMS scanner for dual-axes confocal microscopy. *IEEE J. Microelectromechanical Systems*, 2007; 16:4:969–76
2. Akatay A, Urey H. Design and optimization of microlens array based high resolution beam steering system. *Optics Express* 2000; 15:8: 4523–9, 2007.
3. Duparré J, Radtke D, and Dannberg P. Implementation of field lens arrays in beam-deflecting microlens array telescopes. *Appl. Opt.* 2004; 43: 4854–61.
4. Kwon S, Milanovi V, Lee LP. Large-displacement vertical microlens scanner with low driving Voltage. *IEEE Photonics Technol. Lett.* 2002; 14:11:1572–4.
5. Tuantranont A, Bright VM, Zhang J, Zhang W, Neff JA, Lee YC. Optical beam steering using MEMS-controllable microlens array. *Sensor Actuator. Phys.* 2001;91:3:363–372.
6. Arslan A, Ataman C, Holmstrom S, Hedsten K, Enoksson P, Seren HR, Urey H. Mechanically coupled comb drive MEMS stages. *IEEE Optical MEMS and Nanophotonics*, Freiburg, Germany 2008;140–1.
7. Yalçinkaya AD, Urey H, Brown D, Montague T, Sprague R. Two-axis electromagnetic microscanner for high resolution displays. *IEEE J. Microelectromechanical Systems* 2006; 15:4:786–94.
8. Ataman C, Urey H. Modeling and characterization of comb-actuated resonant microscanners. *J. Micromech. Microeng.* 2006;16: 9–16.